ECRONICON OPEN ACCESS

EC PULMONOLOGY AND RESPIRATORY MEDICINE

Research Article

Calcium Hydroxyapatite and Calcium Pyrophosphate Dihydrate Crystals in Primary Synovial Chondromatosis

Miklós Bély[1]* and Ágnes Apáthy[2]

[1]*Department of Pathology, Hospital of the Order of the Brothers of Saint John of God in Budapest, Hungary*

[2]*Department of Rheumatology, St. Margaret Clinic, Budapest, Hungary*

***Corresponding Author:** Miklós Bély, Department of Pathology, Hospital of the Order of the Brothers of Saint John of God in Budapest, Hungary.

Received: August 19, 2022; **Published:** August 24, 2022

Abstract

Introduction: Primary synovial chondromatosis (prSynCh) is a metaplastic disorder of the synovial membrane, characterized by chondrocyte differentiation of synovial pluripotent stem cells and by marked chondroid and/or osteoid production.

The cause of stem cell differentiation is unknown. Crystal deposits as pathogenic agents are not mentioned in the literature of primary synovial chondromatosis.

Aim of the Study: The aim of this study was to determine the presence of crystal deposits in the synovial membrane by Bély and Apáthy's non-staining technique and to verify the metabolic origin of prSynCh.

Patient Population and Methods: Twenty-one surgical specimens of 20 patients with clinically diagnosed and histologically confirmed primary synovial chondromatosis were studied.

Results and Conclusion: The formal pathogenesis of primary synovial chondromatosis corresponded to the descriptions of the pertinent literature, characterized by clean chondromatosis, mixed osteochondromatosis and pure osteomatosis.

The prSynCh was accompanied by marked hydroxyapatite (HA) and calcium pyrophosphate dihydrate (CPPD) crystal deposits, and was characterized by definite chondroid and/or bone formation. The calcium carbonate [$CaCO_3$] and/or calcium phosphate [$CaPO_4$] deposition was rare and minimal, suggesting an insufficient mineralization capability.

We assume that prSynCh starts with HA and CPPD crystal deposition, which provokes a nonspecific inflammation, with transformation of the pluripotent stem cells into chondrocytes. The conspicuous chondroid and/or osteoid formation replaces the rare and moderate amorphous mineral deposits, and acts as a second line defense mechanism against inflammation provoked by crystalline agents.

In our view the prSynCh is an imperfect metabolic disorder related to apatite rheumatisms or chondrocalcinosis.

Keywords: *Primary Synovial Chondromatosis; Pathogenesis; Calcium Hydroxyapatite; Calcium Pyrophosphate Dihydrate; Apatite Rheumatism; Chondrocalcinosis*

Abbreviations

prSynCh: Primary Synovial Chondromatosis; HE: Hematoxylin Eosin; HA: Calcium Hydroxyapatite - [$Ca_5(PO_4)_3(OH)$]; CPPD: Calcium Pyrophosphate Dihydrate - [$Ca_2P_2O_7.2H_2O$]; MSU: Monosodium Urate Monohydrate [$NaC_5H_3N_4O_3{\cdot}H_2O$] (Monosodium Salt of Uric Acid [$C_5H_4N_4O_3$]); Pr n^0/y: Protocol Number/Year

Introduction

Primary synovial chondromatosis (tenosynovial or bursal chondromatosis, synovial osteochondromatosis, synovial chondrometaplasia, Reichel syndrome or Reichel-Jones-Henderson syndrome - prSynCh) is a metaplastic disorder of the synovial membrane, characterized by chondrocyte differentiation of synovial pluripotent stem cells and chondroid tissue production.

The prSynCh may be accompanied with bone formation, with or without true medullary spaces, and amorphous calcium phosphate [$CaPO_4$] and/or calcium carbonate [$CaCO_3$] deposits.

The cause of stem cell differentiation is unknown; different irritative agents (infective, toxic, mechanic, etc.) are mentioned, but the condition may occur spontaneously as well [1,2].

Crystal deposits as irritative agents of primary synovial chondromatosis due to a clinically latent metabolic disorder are not mentioned in the literature.

Aim of the Study

The aim of this study was to determine the formal pathogenesis of synovial chondromatosis, and to detect crystal deposits in the synovial membrane in order to explore the possible role of crystal induced transformation of stem cells into chondrocytes, i.e., to demonstrate the metabolic origin of prSynCh.

Patient Population and Methods

Surgical specimens (synovial membranes of 14 knees, 5 hips and 2 elbows) of 20 patients with clinically diagnosed and histologically confirmed primary synovial chondromatosis were studied.

Cases of secondary synovial chondromatosis, i.e. due to osteoarthritis, rheumatoid arthritis, aseptic (avascular) bone necrosis, osteochondral traumatic injury, etc. were excluded.

Serial sections (5 microns) of tissue samples were stained with HE [3], Alizarin red S (staining specific for calcium) [4,5] and von Kossa's reaction (specific for phosphate [$CaPO_4$] and carbonate [$CaCO_3$] [4,6].

Conventionally stained tissue sections of surgical specimens were compared with unstained ones according to Bély and Apáthy (2013) [7].

The "non-staining" technique is a very sensitive method, and suitable to identify cholesterol [$C_{27}H_{46}O$], calcium hydroxyapatite [$Ca_5(PO_4)_3(OH)$] (HA), calcium pyrophosphate dihydrate [$Ca_2P_2O_7.2H_2O$] (CPPD) crystals, and is appropriate for the detection of monosodium urate monohydrate [$NaC_5H_3N_4O_3{\cdot}H_2O$] (monosodium salt of uric acid [$C_5H_4N_4O_3$] - MSU) crystals, etc. in formalin fixed, paraffin embedded, unstained tissue sections viewed with polarized light [7-20].

Using Bély and Apáthy's "non-staining" technique [7-20], the fixation of tissue blocks and embedding in paraffin were the same as with the standard staining's and reactions. Unstained tissue sections were deparaffinized, mounted and cover slipped with Canada balsam (description of the method see Appendix below).

Standard and unstained sections were examined with the light microscope (Olympus BX51) and under polarized light, respectively.

Demographics of female and male patients were compared with the student (Welch) t-probe [21].

Appendix - Bély and Apáthy's "non-staining" technique [7-20]:

1. Tissue blocks of surgically removed specimens are fixed in 8% neutral buffered formalin (at pH 7.6 for >24 hours at 20 Co room temperature).
2. Tissue blocks are dehydrated in ethyl alcohol, and are embedded in paraffin using acetone as well as xylene - 5 µm sections are cut.
3. Prolonged deparaffinization (3-5 days) in a thermostat at 56°C (daily changing xylene)
4. Chloroform - methanol I. (1:1) solution for 1 hour
5. Chloroform - methanol II. (1:1) solution for 1 hour or overnight
6. Dehydration in ethyl alcohol (two changes of 96% alcohol I-II. 30-30 min.), and using terpene xylene, as well as xylene, mounting in Canada balsam, cover slip.

Results

Primary synovial chondromatosis affected the synovial membranes of the knee in 14, the hip in 5 and the elbow in 2 of 21 surgical specimens of 20 patients (Figure 1-3).

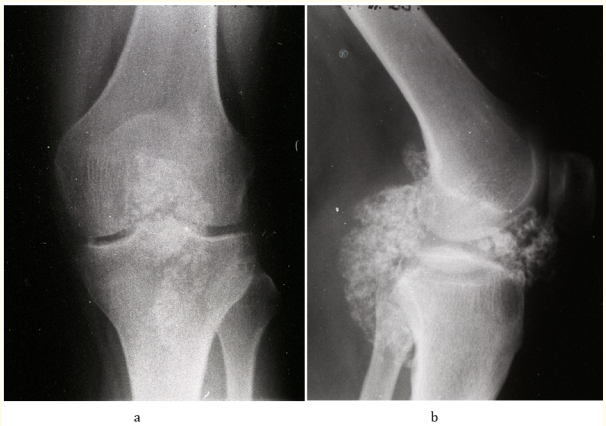

Figure 1: *Legends to figure 1a and 1b (1283/87). Knee, antero-posterior (a) and lateral (b) X-ray, synovial chondromatosis, calcified loose bodies.*

Figure 2: *Legends to figure 2a and 2b (5342/95). Hip, Lauenstein view (a) and antero-posterior radiograph (b), synovial chondromatosis, calcified loose bodies.*

Figure 3: *Legends to figure 3a and 3b (141/1998). Elbow, antero-posterior and lateral X-ray, synovial chondromatosis, calcified loose bodies (ellipse).*

Figure 4-6 are gross photographs of calcified loose bodies and the contact histological sections of a surgical specimen.

Demographics of patients with primary synovial chondromatosis (prSynCh) are summarized in table 1.

There was no significant difference ($p < 0.215$) between female and male patients in mean age of patients at an alpha level of 0.05.

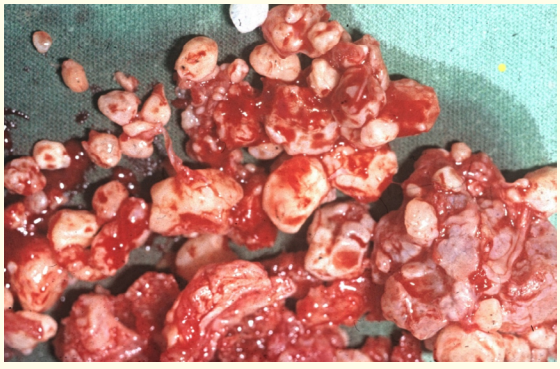

Figure 4: *Legends to figure 4 (2724/93). Synovial chondromatosis, gross photograph of removed calcified and/or ossified loose bodies varying from a few millimeters to a few centimeters in greatest diameter.*

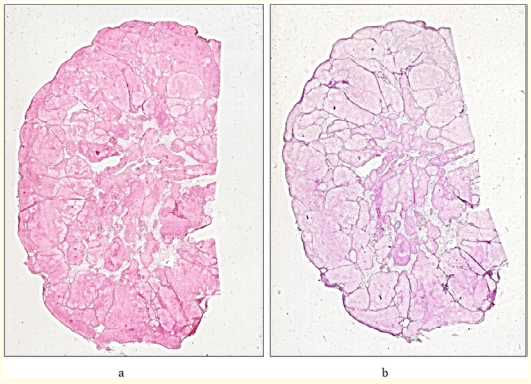

Figure 5: *Legends to figure 5 (126/94). Synovial chondromatosis, contact histological sections of a removed surgical specimen. Islands of newly formed cartilage showed minimal dystrophic calcification (See next figure 6 microscopically). (a) HE, x1, (b) same as (a) PAS, x1.*

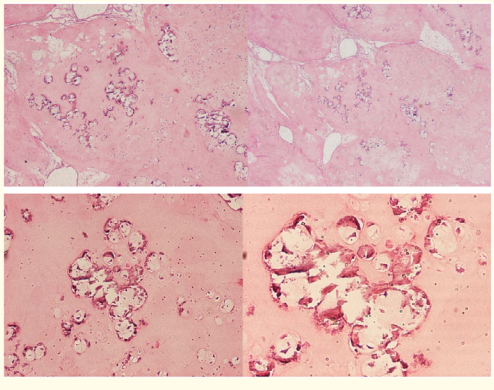

Figure 6: *Legends to figure 6a-6d (126/94). Synovial chondromatosis. The newly formed chondroid nodules are degenerated, partly necrotic, with minimal dystrophic calcification, not to be mistaken for crystal induced mineralization. HE, viewed with the light microscope, x20, (b) same as (a) x40, (c) same as (a) x100, (d) same as (a) x200.*

Gender of patients	Number of patients	Mean age in years at surgery ± SD	Range (In years)
Pts. with primary synovial chondromatosis	20	50.70 ± 12.51	30 - 76
Female	13 of 20	53.15 ± 10.49	40 - 74
Male	7 of 20	44.71 ± 14.90	30 - 76

Table 1: *Sex, mean age with SD, range (in years) of 20 patients with prSynCh.*

Chondromatosis (chondroid formation without osteoid or bone formation) was found in 9, osteochondromatosis (chondroid with osteoid and/or bone formation) in 11, and only bone formation in 1 surgical specimen of 20 patients. True medullary spaces accompanied bone formation in 8 of 12 cases.

Different stages of chondroid, osteoid and/or bone formation existed side by side in the same histologic section.

Minimal or moderate amounts of amorphous calcium phosphate and/or carbonate deposits were present in 12 and were not seen in 8 of 20 patients.

In unstained sections of surgical specimens (n = 7 of 21) HA [$Ca_5(PO_4)_3(OH)$] and CPPD [$Ca_2P_2O_7.2H_2O$] crystals were detected in all cases.

Figure 7-15 demonstrate the formal pathogenesis of prSynCh in conventionally stained sections, viewed with the light microscope, and in unstained ones viewed under polarized light.

Original magnifications of all figures correspond to the 24 x 36 mm transparency slide; the correct height: width ratio is 2:3. The printed size may be different; therefore, the original magnifications are indicated.

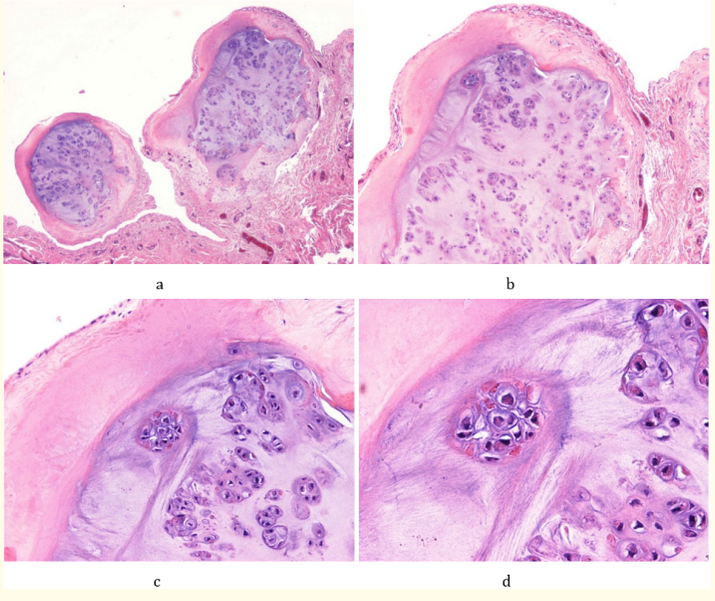

Figure 7: *Legends to figure 7a-7d (501/2015). Synovial chondromatosis, hip joint, nodules of newly formed cartilage, accompanied with minimal calcification of blue-violet color, HE staining. (a) HE, viewed with the light microscope, x20, (b) same as (a) x40, (c) same as (a) x100, (d) same as (a) x200.*

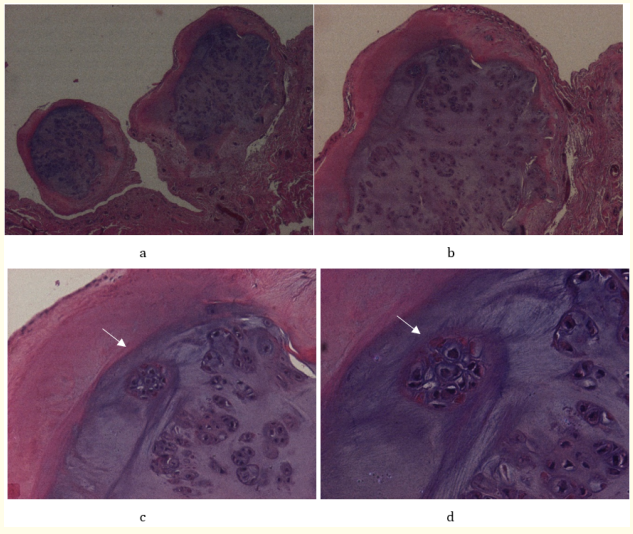

Figure 8: *Legends to figure 8a-8d (same as figure 7a-7d - 501/2015). Synovial chondromatosis, hip joint, nodules of newly formed cartilage, accompanied with minimal calcification. The solubility of HA and CPPD crystals is different in conventional fixatives (aqueous formaldehyde solution), in ethyl alcohol, acetone, xylene and in aqueous solutions of dyes. The more soluble small and weak birefringent HA crystals are virtually non-existent (there is no detectable birefringence) in the HE stained section, while the less soluble large and strongly birefringent CPPD crystals can be preserved and demonstrated with polarized light at high magnification. At high power magnification (c and d) of this figure the CPPD crystals are in close connection to the chondrocytes (arrows). (a) HE, viewed under polarized light, x20, (b) same as (a) x40, (c) same as (a) x100, (d) same as (a) x200.*

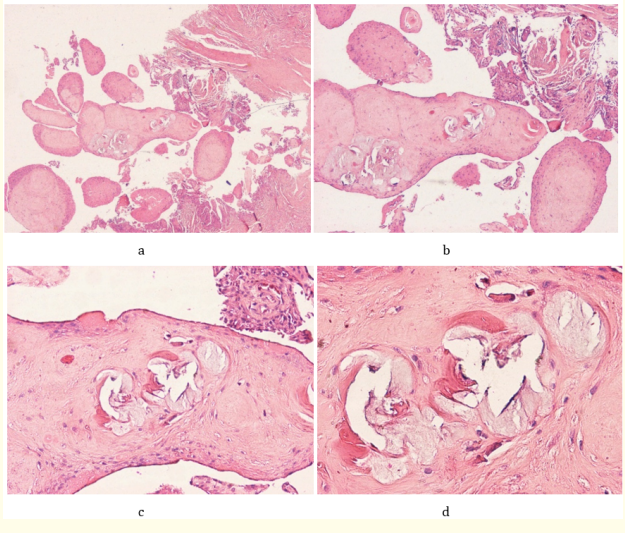

Figure 9: *Legends to figure 9a-9d (1727/2016). Synovial osteo-chondromatosis, knee joint synovial membrane with newly formed chondroid and osteoid nodules. (a) HE, viewed with the light microscope, x20, (b) same as (a) x40, (c) same as (a) x100, (d) same as (a) x200.*

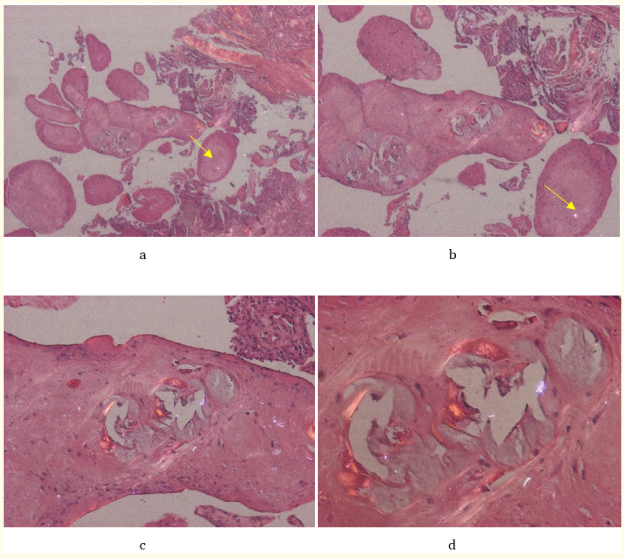

Figure 10: *Legends to figure 10a-10d (same as figure 9a-9d - 1727/2016). Synovial osteo-chondromatosis, knee joint, synovial membrane with newly formed chondroid and osteoid nodules. The less soluble large and strong birefringent CPPD crystals can be preserved and demonstrable by polarized light in traditionally stained sections (arrows). (a) HE, viewed under polarized light, x20, (b) same as (a) x40, (c) same as (a) x100, (d) same as (a) x200.*

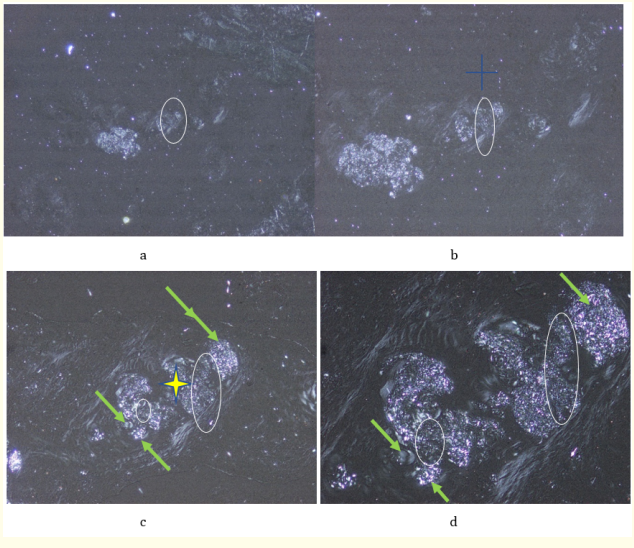

Figure 11: *Legends to figure 11a-11d (same as figure 9a-9d - 1727/2016). Synovial osteo-chondromatosis, knee joint, synovial membrane with newly formed chondroid and osteoid nodules, unstained sections with mixed HA and CPPD crystal deposits, viewed under polarized light. The HA crystals are colorless, translucent fragments or small (50-500 nm), rod-shaped prisms, with weak birefringence (white ellipse). The CPPD crystals are submicroscopic to 40 µm, rhomboid, strongly birefringent crystals (green arrows). (a) unstained sections, viewed under polarized light, x20, (b) same as (a) x40, (c) same as (a) x100, (d) same as (a) x200.*

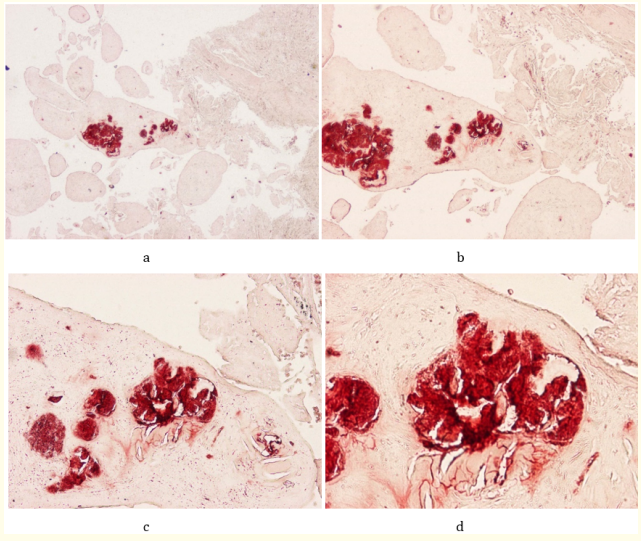

Figure 12: *Legends to figure 12a-12d (same as figure 9a-9d - 1727/2016). Synovial osteo-chondromatosis, knee joint synovial membrane with newly formed chondroid and osteoid nodules, stained by calcium specific Alizarin red S, viewed with the light microscope. The HA and CPPD crystals are accompanied with minimal amorphous calcium phosphate [CaPO4] and/or calcium carbonate [CaCO3] deposits. Amorphous mineral deposits mask the crystals. (a) Alizarin red S staining, viewed with the light microscope, x20, (b) same as (a) x40, (c) same as (a) x100, (d) same as (a) x200.*

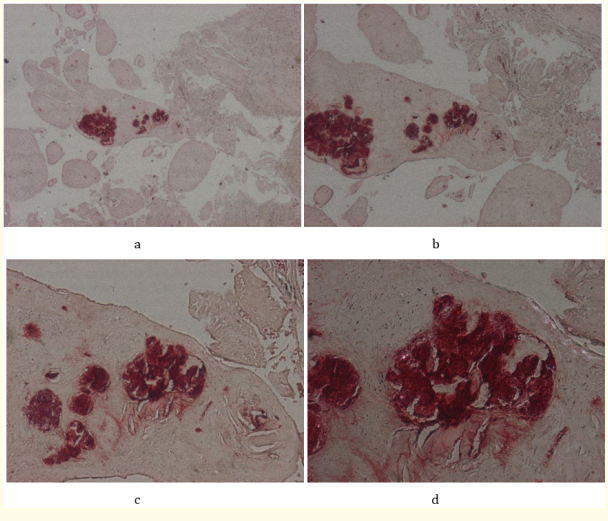

Figure 13: *Legends to figure 13a-13d (same as figure 9a-9d - 1727/2016). Synovial osteo-chondromatosis, knee joint synovial membrane with newly formed chondroid and osteoid nodules, stained by calcium specific Alizarin red S, viewed under polarized light. The HA and CPPD crystals are accompanied with minimal amorphous calcium phosphate [CaPO4] and/or calcium carbonate [CaCO3] deposits. Amorphous mineral deposits mask the crystals; no detectable birefringence. (a) Alizarin red S staining, viewed under polarized light, x20, (b) same as (a) x40, (c) same as (a) x100, (d) same as (a) x200.*

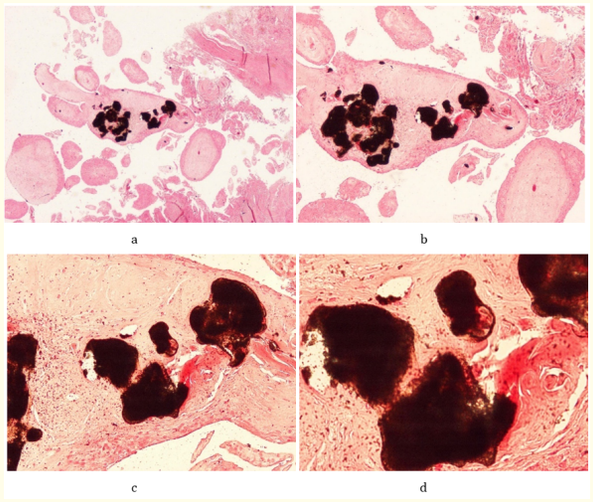

Figure 14: *Legends to figure 14a-14d (same as figure 9a-9d - 1727/2016). Synovial osteo-chondromatosis, knee joint, synovial membrane with newly formed chondroid and osteoid nodules, stained for phosphate or carbonate specific von Kossa reaction, viewed with the light microscope. The HA and CPPD crystals are accompanied with minimal amorphous calcium phosphate [CaPO4] and/or calcium carbonate [CaCO3] deposits. Amorphous mineral deposits mask the crystals; without detectable birefringence. (a) von Kossa reaction, viewed with the light microscope, x20, (b) same as (a) x40, (c) same as (a) x100, (d) same as (a) x200.*

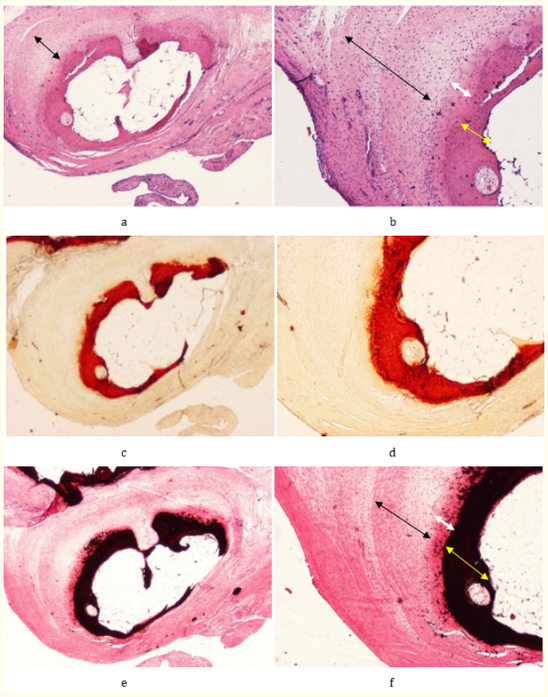

Figure 15: *Legends to figure 15a-15f (431/2016). Synovial osteo-chondromatosis, knee joint, nodules composed of newly formed cartilage (black arrow), osteoid (white arrow) and bone (yellow arrow), with true medullary spaces, stained by HE, calcium specific Alizarin red S, and phosphate or carbonate specific von Kossa reaction, viewed with the light microscope. The newly formed calcified bone tissue stain with calcium specific Alizarin red S, and with von Kossa reaction specific for phosphate or carbonate. (a) HE, x20, (b) same as (a) x40. (c) Alizarin red S staining, same as (a) x20, (d) same as (c) x40. (e) von Kossa reaction, same as (a) x20, (f) same as (e) x40.*

Table 2 summarizes the amount of HA and CPPD crystals in non-stained sections in relation to the amorphous calcium phosphate or carbonate deposits in patients with clinically diagnosed primary synovial chondromatosis.

Clinical diagnosis	HA [$Ca_5(PO_4)_3(OH)$] crystal deposits	CPPD [$Ca_2P_2O_7.2H_2O$] crystal deposits	[$CaPO_4$] or [$CaCO_3$] stained by HE, Alizarin red S or von Kossa reaction
Synovialis chondromatosis			
1535/89 (left knee) synovial membrane	More than 90%	Less than 10%	None
126/94 (knee) synovial membrane	Less than 10%	More than 90%	Minimal
2569/2008 (right knee) synovial membrane	More than 90%	Less than 10%	None
501/2015 (left hip) synovial membrane	More than 90%	Scattered sporadic	Minimal
1214/2015 (left hip) head of femur, synovial membrane	50%	50 %	Minimal
431/2016 (left knee) synovial membrane	Less than 20%	More than 80 %	Moderate
1727/2016 (right knee) synovial membrane	50 %	50 %	Moderate

Table 2: *Presence and amount of HA and CPPD crystals, with or without amorphous calcium phosphate or carbonate deposits in primary synovial chondromatosis.*

Remark to table 2

Primary synovial chondromatosis was diagnosed clinically and confirmed histologically.

The marked chondroid and/or bone formation is characteristic for prSynCh, accompanied usually only with minimal amorphous mineral deposits.

In one patient the same hip was operated two times: Pr n^0/y 501/2015 (Synovectomy, 29.01.2015.), and 1214/2015 (TEP with rest of synovial membrane, 13.04.2015).

HA [$Ca_5(PO_4)_3(OH)$] or CPPD [$Ca_2P_2O_7.2H_2O$] crystal deposits were demonstrated with the non-staining techniques of Bély and Apáthy (2013).

Only seven surgical specimens of 6 patients were available for retrospective analysis of HA and CPPD crystals deposits in non-stained sections.

The size of individual HA crystals is submicroscopic [22], according to others 50-500 nm [23], in clusters 1-5 µm [23] or 1.9-15.6 µm [24].

In apatite rheumatism the HA crystal clusters "tend to aggregate into globular clumps, and can appear as refractile shiny coins on light microscopy, but show no birefringence under compensated polarized microscopy (400 x)" with traditional stains [25].

Using a professional polarizing microscope with high, at least 100-Watt brightness the HA crystal clusters (1-5 µm) are visible and birefringent with polarized light (100x), moreover they can form larger aggregates (conglomerates) of 100 µm or larger, which are visible with an objective of 40x by non-staining techniques [14,15].

The birefringence of HA crystals is weak compared to the strong birefringence of CPPD crystals; the strongly birefringent CPPD crystals can be deceptively dominate the microscopic fields (Figure 11 and 17).

CPPD crystals are less soluble in 8% aqueous formaldehyde solution and in aqueous solutions of dyes than HA crystals; variable amounts of CPPD crystals can be occasionally preserved in tissue sections, and remain demonstrable in conventionally fixed tissues stained with HE, Alizarind red S or von Kossa's reaction.

In unstained sections viewed under polarized light the CPPD crystals have a rhomboid shape (Figure 11 and 17). The expected size range is 0.42 - 17.9 µm [26], according to others it varies from submicroscopic to 40 µm [24].

With Red I compensator the CPPD crystals show a strong positive birefringence, in contrast to the weak positive birefringence of HA crystals (Figure 17 and 18).

Amounts of HA and CPPD may vary per foci side by side within one tissue section and may be accompanied with more or less amorphous mineral deposits.

Calcium carbonate [$CaCO_3$] and/or calcium phosphate [$CaPO_4$] deposits were demonstrated in serial sections of surgical specimens with HE, Alizarin red S staining or von Kossa reaction.

Figure 16 demonstrate the electron microscopic characteristics of HA or CPPD crystals, viewed by surface electron microscope (JEM 100CX) in patients with clinically diagnosed apatite rheumatism or chondrocalcinosis.

The original magnification of electron microphotographs corresponds to the 60 x 90 mm negatives.

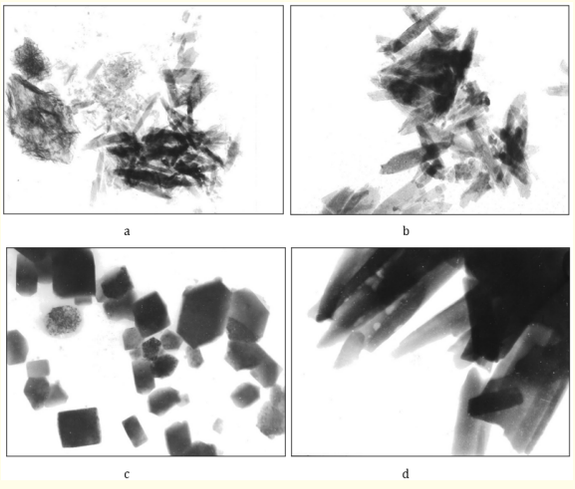

Figure 16: *Legends to figure 16a-16d. Electron microscopic characteristics of HA and CPPD crystals in surgical specimens of patients with the clinical diagnosis of apatite rheumatism and chondrocalcinosis. (a) Clusters of rod-shaped HA crystals, surface electron micrograph, x20000, (b) rod-shaped HA crystals, surface electron micrograph, x50000, (c) plates of CPPD crystals, surface electron micrograph, x10000, (d) rod-shaped CPPD crystals, surface electron- micrograph, x10000.*

Figure 17-20 demonstrate the histological characteristics of HA or CPPD crystal deposits in unstained sections, viewed under polarized light.

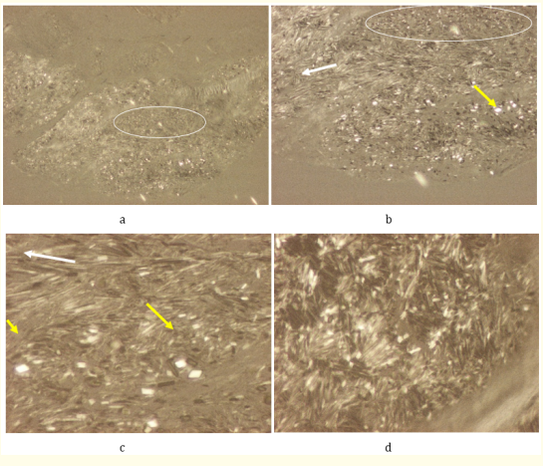

Figure 17: *Legends to figure 17a-17d (431/2016). Synovial osteo-chondromatosis, knee joint, synovial membrane with weak birefringent HA (white ellipse), and strong birefringent CPPD crystals side by side. The CPPD crystals are rod-shaped (white arrows) or rhomboid (yellow arrows). Their size ranges from 0.42 to17.9 µm [26], according to others it varies from submicroscopic to 40µm [24]. The CPPD crystals parallel to each other and may show in the same position positive or negative (black or white) birefringence, turned around their long axis (white arrow). (a) Unstained sections, viewed under polarized light, x100, (b) same as (a) x200, (c) same as (a) x600, (d) same as (a) x600.*

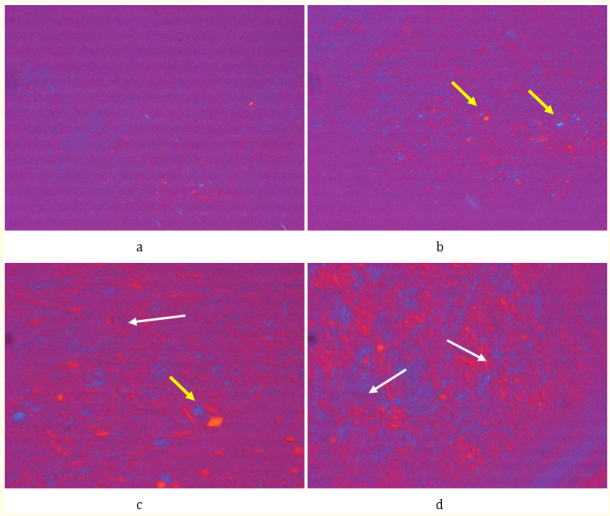

Figure 18: *Legends to figure 18a-18d (same as figure 17a-17d - 431/2016). Synovial osteo-chondromatosis, knee joint, synovial membrane, with weakly birefringent HA and strongly birefringent CPPD crystals (yellow arrows) side by side. The Red I compensator particularly reduced the brightness of illumination (the crystals are less brilliant). The weak illumination deceptively amplifies the presence of strongly birefringent CPPD crystals, in contrast to HA crystals. The CPPD crystals are typically rhomboid (yellow arrows) or rod-shaped (white arrows), with a positive birefringence. The parallel settled CPPD crystals may show positive and negative birefringence in the same position, turned around their long axis. (a) Unstained sections, viewed under polarized light, using Red I compensator, same fields as (16a-16d) x100, (b) same as (a) x200, (c) same as (a) x600, (d) same as (a) x600.*

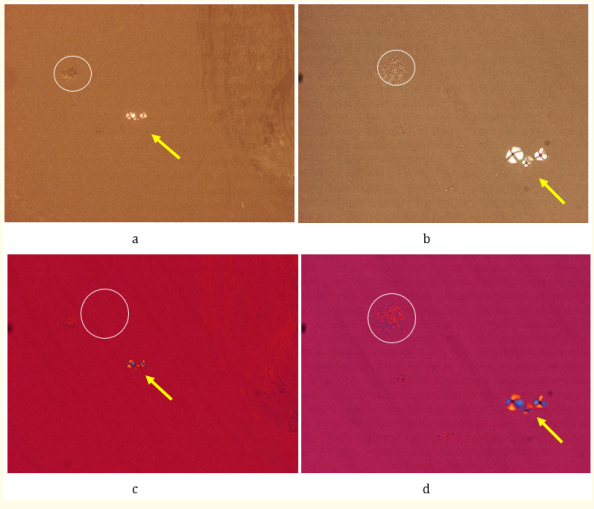

Figure 19: *Legends to figure 19a-19d (2569/2008). Synovial osteo-chondromatosis, knee joint, synovial membrane, early stage of HA crystal deposition. The rod-shaped prisms of HA crystals are arranged in spheroid microaggregates (white ellipse). Under polarized light the direction of birefringence is positive according to the long axis of HA crystals, like that of talcum (yellow arrow). The size of HA crystals in clusters is 1 - 5 µm [23] or 1.9 - 15.6 µm [24], and the size of talcum is 2 - 5 µm [24]. (a) Unstained sections, viewed under polarized light, x100, (b) same as (a) x200, (c) Unstained sections, viewed under polarized light, using Red I compensator, same fields as (a) x100, (d) same as (c) x200.*

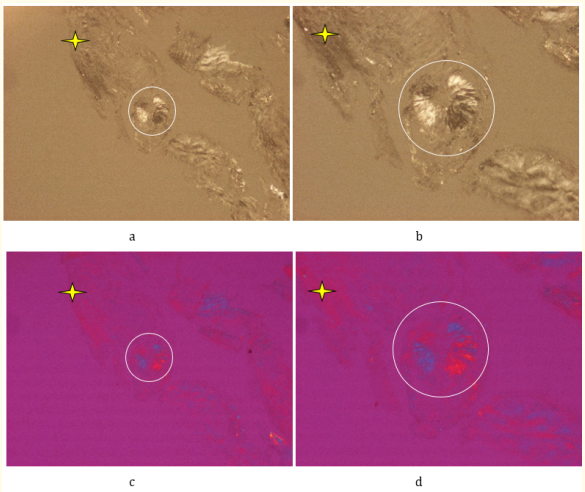

Figure 20: *Legends to figure 20a-20d (431/2016). Synovial osteo-chondromatosis, knee joint synovial membrane, advanced stage of HA crystal deposition. The rod-shaped prisms of HA crystals are arranged in larger spheroid microaggregates (white ellipse). Under polarized light the direction of birefringence is positive according to the long axis of HA crystals, like that of collagen fibers (yellow star). (a) Unstained sections, viewed under polarized light, x100, (b) same as (a) x200, (c) Unstained sections, viewed under polarized light, using Red I compensator, same fields as (a) x100, (d) same as (c) x200.*

Figure 21 demonstrates the characteristic morphology of individual CPPD crystals.

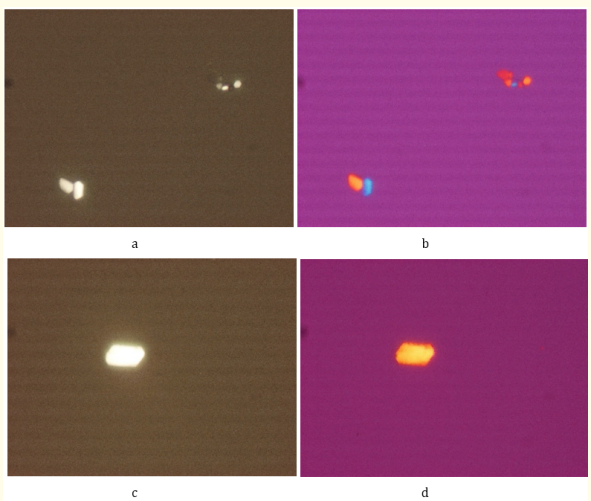

Figure 21: *Legends to figure 21a-21d (126/1994). Synovial chondromatosis, knee joint, synovial membrane, with strong birefringent plane CPPD crystals. CPPD is typically a plane crystal with positive birefringence; hexagonal. rhomboid, trapezoid, parallelogram-shaped or fragments of these. (a) CPPD crystals, unstained sections, viewed under polarized light, x600, (b) CPPD crystals, unstained sections, using Red I compensator, same fields as (a) x600, (a) CPPD crystals, unstained sections, viewed under polarized light, x600, (b) CPPD crystals, unstained sections, using Red I compensator, same fields as (a) x600.*

Discussion

Primary synovial chondromatosis is characterized by slow progression of symptoms, joint pain, and swelling, stiffness, limited motion of affected joint, intraarticular fluid, tenderness and creaking, grinding, or popping noise during movement (crepitus) or locking of the joint [1,2].

The prSynCh occurs most often in the knee joint, followed by the hip, elbow, and shoulder joints [1], but any joints can be affected [2], such as the temporomandibular [27,28], ankle [29], subtalar [30] etc [31]. Bilateral involvement of the joints is uncommon, but may occur [32].

In agreement with the literature, the prevalence of prSynCh was similar in our patients' cohort; the knee was affected in 14, the hip in 5 and the elbow in 2 cases of 21 patients.

According to the literature the mean age of patients is most often between 30 and 50 years, and men are affected by prSynCh twice as often, as women [1].

In contrast with these data, the range of mean age of our patients was between 30 and 76 years. There was no significant difference in the mean age between females and males ($p < 0.215$), and women were nearly twice often affected than men (13 versus 7).

Treatment for synovial chondromatosis is typically observation of the asymptomatic cases, analgesics, and later on surgery to remove the loose bodies according to their size and number, with or without synovectomy (depending on the condition of synovial membrane) [1].

The use of steroids is recommended only as a second line treatment [33].

The formal pathogenesis of primary synovial chondromatosis in our surgical specimens corresponded to the descriptions in the literature characterized by clean chondromatosis, mixed osteochondromatosis, and pure osteomatosis [34] (Figure 7-15).

The mineralization pattern of prSynCh is poorly understood [35].

Matsumura., *et al*. (2014) demonstrated calcium pyrophosphate dihydrate (CPPD) crystals in primary synovial chondromatosis [28].

According to our best knowledge calcium hydroxyapatite [$Ca_5(PO_4)_3(OH)$] (HA) crystals are not mentioned in connection with prSynCh, except our earlier publication [18].

HA crystals are small, rod shaped, weak birefringent, and in conventionally stained sections show no detectable birefringence viewed under polarizing light [25]. The HA crystals are well demonstrable with the non-staining technique of Bély and Apathy's, using a professional polarizing microscope with high, at least 100 Watt brightness [7,9-19].

The hip joint in one of our patients was operated twice, with an interval of 13 weeks.

In the synovial membrane removed at the first operation (501/2015) the HA crystals dominated (> 90%) versus CPPD crystals (< 10%). In the rest of the synovial membrane removed three months later (1214/2015) the ratio of HA and CPPD crystals was practically the same (50 - 50%), supporting the view that crystal deposition starts with the HA, followed later by multiple CPPD deposits [19].

In both cases the amount of calcium phosphate [$CaPO_4$] and/or calcium carbonate [$CaCO_3$] deposition was minimal, suggesting that the amorphous mineral deposition occurs later following the deposition of crystals.

Considering all analyzed cases, dominant (> 90%) HA crystal deposition was not accompanied by amorphous mineral deposits in two patients (1535/89 and 2569/2008), and in a third patient (501/2015) non-crystalline mineralization was only minimal.

In contrast with HA, the increasing CPPD crystal deposits were associated with minimal (126/1994 and 1214/2015) or moderate (431/2016 and 1727/2016) deposits, i.e. with greater amounts of amorphous minerals, which supports also the view that calcium phosphate or carbonate deposition occurs later, following the HA and CPPD crystal deposition [19].

We consider the deposition of amorphous [$CaPO_4$] or [$CaCO_3$] a tissue defense mechanism which inhibits (moderates) the crystal-provoked inflammatory reaction of the involved joint, caused by the CPPD crystals [19].

Since the basic metabolic disorder is still existing, the pathological processes progress, and affect further joints or synovial membranes, such as bursae [36], tendon sheets [37] etc. and thus prSynCh becomes a polyarticular malady.

In each case, the indication for surgery is determined by the joint complaints, mostly by the symptoms of the knee joint [1].

prSynCh was accompanied by marked HA and/or CPPD deposits and can be considered as a combined or coexistent disorder; combined or coexistent synovial chondromatosis and apatite rheumatism (1535/89, 2569/2008, 501/2015) or combined or coexistent chondromatosis and chondrocalcinosis (126/1994, 431/2016), while the rest of the cases (1214/2015, 1727/2016) can be considered mixed forms of these.

In our previous study we concluded, that "apatite rheumatism" and "chondrocalcinosis" are different stages of the same, crystal induced metabolic disorder, accompanied in most cases by abundant calcium phosphate [$CaPO_4$] and/or calcium carbonate [$CaCO_3$] deposits, while the chondroid and/or osteoid formation is unusually rare and minimal [19].

The prSynCh is characterized by conspicuous chondroid and/or bone formation in contrast to apatite rheumatism or chondrocalcinosis, while calcium carbonate [$CaCO_3$] and/or calcium phosphate [$CaPO_4$] deposition is unusually rare and minimal.

These differences suggest that prSynCh and apatite rheumatism or chondrocalcinosis are related, but distinct metabolic diseases, which belong to the same group of metabolic maladies.

Both of these diseases start with HA crystal deposits followed by CPPD crystals, which provoke of inflammatory reaction.

The inflammatory reaction is inhibited or moderated by calcium carbonate [$CaCO_3$] and/or calcium phosphate [$CaPO_4$] deposition in case of apatite rheumatism or chondrocalcinosis and inhibited or moderated by chondroid and/or osteoid formation in case of prSynCh.

Among these disorders the key factor is the production of amorphous minerals; in apatite rheumatism or chondrocalcinosis the production is given and in case of prSynCh it is not. This ability can be determined by genetic or other, unidentified factors.

Conclusion

The exact sequence and nature of the mineralization processes accompanying prSynCh is unclear.

We assume that the pre-chondromatous phase of prSynCh starts with hydroxyapatite (HA) and calcium pyrophosphate dihydrate (CPPD) crystal deposition, provoking the transformation of pluripotent stem cells into chondrocytes, leading to chondroid and/or osteoid production, in case of insufficient mineralization capabilities.

We consider prSynCh essentially a defective metabolic disorder with reduced mineralization capabilities, in contrast to chondrocalcinosis or apatite rheumatism.

The difference between these diseases is only recognizable in the prevalence and amount of chondroid and/or osteoid formation, respectively in the prevalence and amount of amorphous calcium phosphate and/or carbonate production.

In our opinion the prSynCh, apatite rheumatisms and chondrocalcinosis are related maladies, and belong to the same group of metabolic diseases.

Bibliography

1. "Synovial Chondromatosis - OrthoInfo - AAOS.
2. Synovial Chondromatosis - GARD.
3. Carson FL. "Mayer's hematoxylin" In: Histotechnology (Editor: Carson FL), ASCP Press: Chicago (1990): 100-103.
4. McManus JFA and Mowry RW. "Methods of general utility for the routine study of tissues", "Sodium Alizarin sulfonate stain for calcium" and "Von Kossa's method for phosphates and carbonates". In: Staining methods, histologic and histochemical (Editors: McManus JFA, Mowry RW), Hoeber PB Inc, New York (1960): 55-72.
5. Vacca LL. "Alizarin red S" In: Laboratory manual of histochemistry (Editor: Vacca LL), Raven Press, New York (1985): 333-334.
6. Lillie RD. "Von Kóssa's method". In: Histopathologic technic and practical histochemistry (Editor: Lillie RD), The Blakiston Division McGraw-Hill Book Company, New York, Toronto, London (1954): 264-265.
7. Bély M and Apáthy Á. "Mönckeberg sclerosis - kristály indukálta angiopathia (Mönckeberg‟s sclerosis: crystal-induced angiopathy)". *Orvosi Hetilap* 154.23 (2013): 908-913.
8. Bély M and Krutsay M. "A simple method to demonstrate urate crystals in formalin fixed tissue". *Journal of Autoimmune Diseases and Rheumatology (JADR)* 1 (2013): 46-49.
9. Bély M and Apáthy A. "Functional Role of Hydroxyapatite Crystals in Mönckeberg's Arteriosclerosis". *Journal of Cardiovascular Disease (JCvD)* 2.5 (2014): 228-234.
10. Bély M Apáthy Ágnes. "A microscopic method for identification of calcium pyrophosphate dihydrate deposits in tissues". *Annals of the Rheumatic Diseases* 73 (2014): 1061.
11. Bély M and Apáthy Á. "A Simple Method for the Microscopic Identification of Calcium Pyrophosphate Dihydrate and Hydroxyapatite Deposits in Metabolic and Crystal Induced Diseases". *Annals of the Rheumatic Diseases* 73 (2014): 1081.
12. Bély M and Apáthy Á. "Calcium Pyrophosphate Dihydrate and Hydroxyapatite Crystal Induced Metabolic Diseases – Same or Different?" *Annals of the Rheumatic Diseases* 75 (2016): 1184.

13. Bély M and Apáthy Á. "A Simple Method of Diagnostic Pathology for Identification of Crystal Deposits in Metabolic and Crystal Induced Diseases". *Structural Chemistry and Crystallography Communication* 2 (2016): 1-15.

14. Bély M and Apáthy A. "Metabolic Diseases and Crystal Induced Arthropathies Technic of Non-Staining Histologic Sections - A Comparative Study of Standard Stains and Histochemical Reactions". *Clinical Archives of Bone and Joint Diseases* (2018): 1.2.

15. Bély M and Apáthy A. "Crystal deposits in tissue of patients with chondrocalcinosis and apatite rheumatism - Microscopic identification of CPPD and HA with the non-staining technique of Bely and Apáthy". *BAOJ Clinical Trials* 4 (2016): 018.

16. Bély M and Balogh K. "Calcification and crystal deposition of aortic valves in clinically latent metabolic disease – A case report". *EC Cardiology* 8.6 (2021): 40-47.

17. Bély M and Apáthy Á. "Vascular calcification and crystal deposition diseases - A comparative study on 67 amputated legs with atherosclerosis and/or Mönckeberg sclerosis". *EC Cardiology* 8.10 (2021): 01-19.

18. Bély M and Apáthy A. "Crystal deposits in primary synovial chondromatosis". *Annals of the Rheumatic Diseases* 81.1 (2022): 1642.

19. Bély M and Apáthy A. "Crystal deposits in apatite rheumatism and chondrocalcinosis – microscopic identification of hydroxyapatite and calcium pyrophosphate dihydrate crystals with standard stains and histochemical reactions and with the nonstinging technique of Bély and Apáthy". *EC Pulmonology and Respiratory Medicine* 11.5 (2022): 03-24.

20. Bély M and Apáthy A. "Crystal deposits in tissue of 64 patients with gout - A comparative study of standard stains and histochemical reactions with the non-staining technique of Bély and Apáthy". *EC Cardiology* 9.4 (2022): 01-19.

21. Lentner C. "Statistical methods". In Geigy scientific tables, 8th revised and enlarged edition: Ciba-Geigy Limited, Basle, Switzerland, Editor: Lentner C, Compiled by: Diem K, Seldrup J 2 (1982): 227.

22. Swan A., *et al*. "Submicroscopic crystals in osteoarthritic synovial fluids". *Annals of the Rheumatic Diseases* 53.7 (1994): 467-470.

23. Pay S and Terkeltaub R. "Calcium pyrophosphate dihydrate and hydroxyapatite crystal deposition in the joint: New developments relevant to the clinician". *Current Rheumatology Reports* 5.3 (2003): 235-243.

24. Gatter RA and Schumacher HR. "Microscopic findings under compensated polarized light and phase light". In: A practical handbook of joint synovial fluid analysis (Editors: Gatter RA, Schumacher HR), 2nd edition.: Lea and Febiger, Philadelphia, London (1991): 46.

25. Reginato AM and Yuvienco C. "Hydroxyapatite Crystal-Induced". Rheumatology (2017).

26. Uhthoff HK and Loehr JW. "Calcific Tendinopathy of the Rotator Cuff: Pathogenesis, Diagnosis, and Management". *Journal of the American Academy of Orthopaedic Surgeons* 5.4: 183-191.

27. Mandrioli S., *et al*. "Synovial Chondromatosis of the Temporomandibular Joint". *Journal of Craniofacial Surgery* 18.6 (2007): 1486-1488.

28. Y Matsumura., *et al*. "Synovial chondromatosis of the temporomandibular joint with calcium pyrophosphate dihydrate crystal deposition disease (pseudogout)". *Dermatomaxillofacial Radiology* 41.8 (2014): 703-707.

29. Sedeek M., *et al*. "Synovial Chondromatosis of the Ankle Joint: Clinical, Radiological, and Intraoperative Findings". *Case Reports in Orthopedics* (2015).

30. Stensby JD., *et al*. "Primary synovial chondromatosis of the subtalar joint: case report and review of the literature". *Skeletal Radiology* 47.3 (2018): 391-396.

31. Baecher NB. "Synovial Chondromatosis". Medscape, Synovial Chondromatosis (2020).

32. Mo J., *et al*. "Bilateral synovial chondromatosis of the elbow in an adolescent: a case report and literature review". *BMC Musculoskeletal Disorders* 21 (2020): 377.

33. Pálinkás M and Poór Gy. "Kristályatrthritisek". In Reumatológia (Editors: Szekanecz Z, Nagy Gy). Medicina könyvkiadó Zrt. Budapest 41 (2019): 572.

34. Mohr W. "Primare synoviale Osteochondromatose". 14.1.2, In: Mohr W, Gelenkpathologie, historische Grundlagen, Ursachen und Entwicklungen von Gelenkleiden und ihre Pathomorphologie. (1st edition), Springer-Verlag, Berlin, Heidelberg, Germany (2000): 496-501.

35. Beger AW., *et al*. "Primary synovial chondromatosis: an elemental investigation of a rare skeletal pathology". *Folia Morphologica* (2021).

36. Borges AM., *et al*. "Bursa Formation and Synovial Chondrometaplasia Associated with Osteochondromas". *American Journal of Clinical Pathology* 75.5 (1981): 648-653.

37. Shankar V. "Synovial and tenosynovial chondromatosis". *Pathology Outlines* (2022).

Volume 11 Issue 8 August 2022